Kinematic Structure Correspondences via Hypergraph Matching <Supplementary Material>

Hyung Jin Chang Tobias Fischer Maxime Petit Martina Zambelli Yiannis Demiris
Department of Electrical and Electronic Engineering
Imperial College London, United Kingdom
{hj.chang, t.fischer, m.petit, m.zambelli13, y.demiris}@imperial.ac.uk

1. Validations on Parameters of VF2

As shown in Table 1, we did not find a significant performance difference between $\theta = 1$ and $\theta = 2$, and decreases for $\theta \geq 2$. For the local constraint, θ typically varies between 1 and 2. Values outside this range do not seem plausible, as the skeleton would need to be highly distorted. The impact of the global constraint τ is low, as the difference in the total edge degree is used as a quality measure. Thus, even if τ is increased, the newly found subgraph isomorphisms have low weight (Eq(3)). Experimentally, we found that τ does not affect the performance for $\tau \geq 3$. However, $\tau = 1$ or $\tau = 2$ prohibits correct graph matching and decreases performance.

Table 1. Validations on the parameters of VF2.

Parameter		Accuracy (%)
τ	θ	
3	1	92.99 ($\pm$10.41)
3	2	91.26 ($\pm$11.32)
3	3	88.23 ($\pm$19.83)
3	4	88.23 ($\pm$19.83)
2	1	81.30 ($\pm$29.32)
4	1	92.99 ($\pm$10.41)
5	1	92.99 ($\pm$10.41)
6	1	92.99 ($\pm$10.41)
2	2	85.19 ($\pm$28.62)
4	2	91.26 ($\pm$11.32)
5	2	91.26 ($\pm$11.32)
6	2	91.26 ($\pm$11.32)

2. Experimental Results

We provide additional experimental results of Section 4.2 of our main paper which was not able to be included due to the page limit.

2.1. Real Kinematic Structure Dataset

In the experiments of Section 4.2, we have shown comparisons with graph alignment methods and object appearance based methods. In Figures 1 to 9 of this supplementary document, we additionally show correspondence matching results using different hypergraph matching methods with the proposed similarity function. Furthermore, we present all comparisons which were not included in Figure 5 of the main paper because of the page limit. In particular, concerning the results of PGM method [2], we show the 50 highest scoring matches for a better comparison.

2.2. Symmetric Kinematic Structure Results

In Figure 5 of the main paper, we briefly mentioned upside-down matches between two iCub robots. In Figure 10 and 11 of this supplementary document, we present image sequences of the pairs in order to demonstrate their motion directions. From these results, it can be observed that the proposed combinatorial motion similarity term is able to imply motion directions.

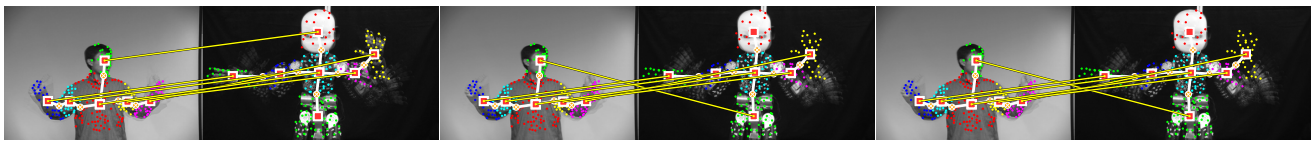

(a) Proposed (b) Graph alignment: NETAL [5] (c) Graph alignment: MAGNA++ [7]

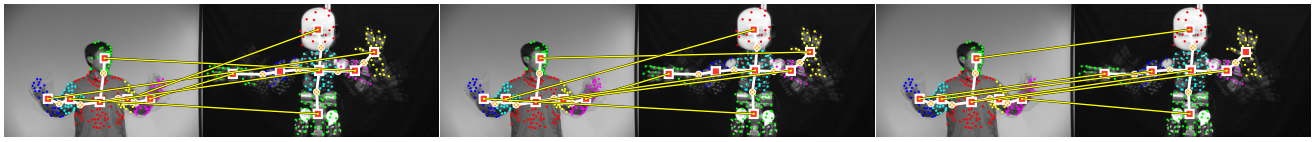

(d) Proposed $\mathcal{F}$ to TM [3] (e) Proposed $\mathcal{F}$ to HGM [8] (f) Proposed $\mathcal{F}$ to BCAGM+MP [6]

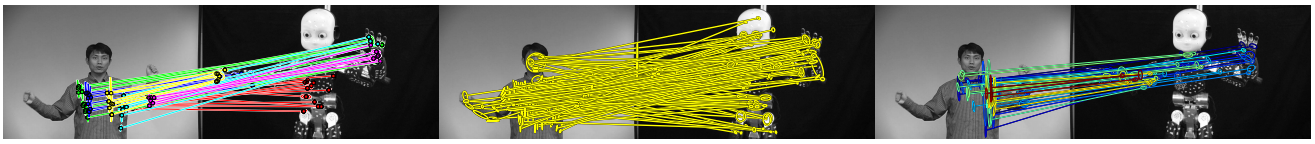

(g) Appearance feature matching: ACC [1] (h) Appearance feature matching: RRWM [4] (i) Appearance feature matching: PGM [2]

Figure 1. Experiments on real image datasets: dancing human *vs.* dancing iCub (best viewed in colour).

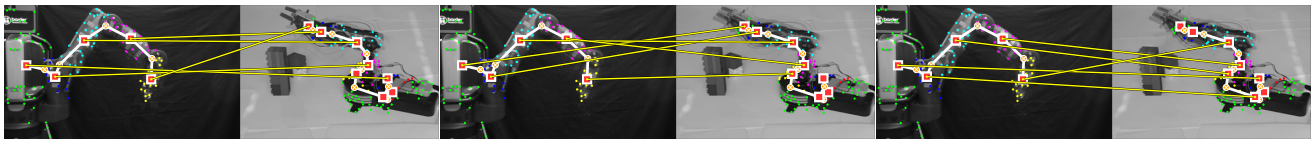

(a) Proposed (b) Graph alignment: NETAL [5] (c) Graph alignment: MAGNA++ [7]

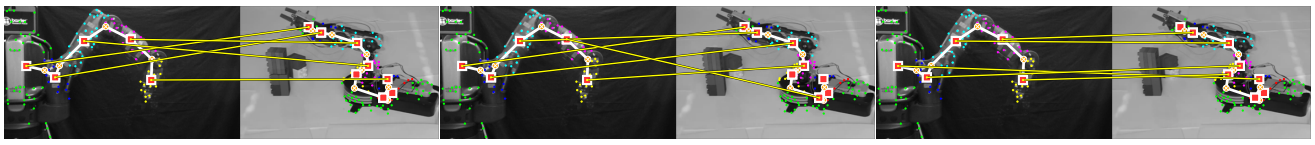

(d) Proposed $\mathcal{F}$ to TM [3] (e) Proposed $\mathcal{F}$ to HGM [8] (f) Proposed $\mathcal{F}$ to BCAGM+MP [6]

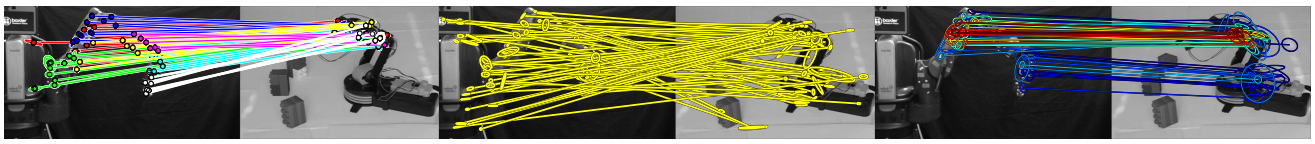

(g) Appearance feature matching: ACC [1] (h) Appearance feature matching: RRWM [4] (i) Appearance feature matching: PGM [2]

Figure 2. Experiments on real image datasets: Baxter *vs.* OWI-535 Robotic Arm Edge (best viewed in colour).

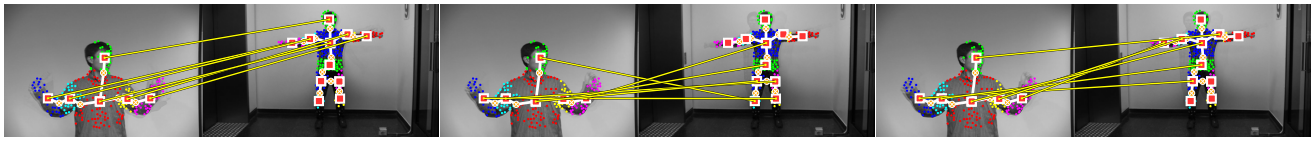

(a) Proposed (b) Graph alignment: NETAL [5] (c) Graph alignment: MAGNA++ [7]

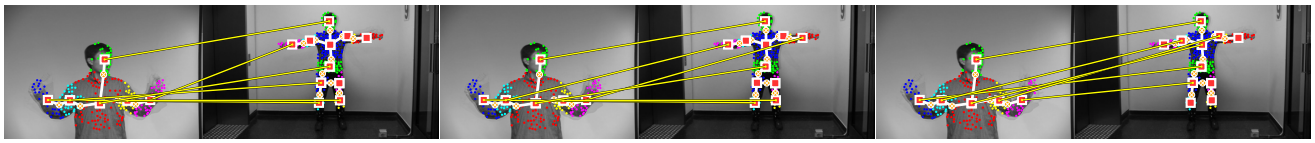

(d) Proposed $\mathcal{F}$ to TM [3] (e) Proposed $\mathcal{F}$ to HGM [8] (f) Proposed $\mathcal{F}$ to BCAGM+MP [6]

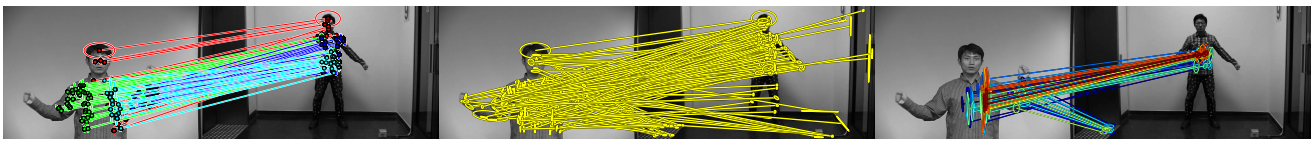

(g) Appearance feature matching: ACC [1] (h) Appearance feature matching: RRWM [4] (i) Appearance feature matching: PGM [2]

Figure 3. Experiments on real image datasets: dancing human *vs.* human full body (best viewed in colour).

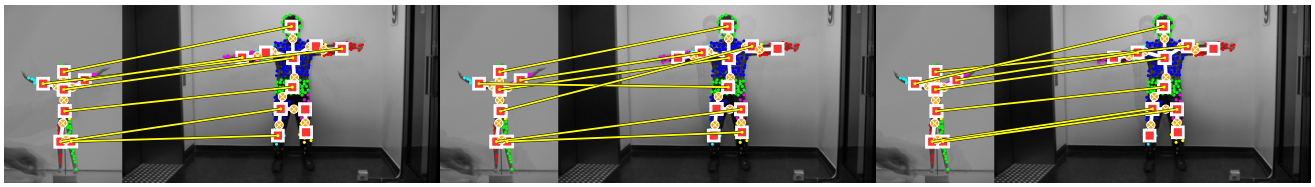

(a) Proposed (b) Graph alignment: NETAL [5] (c) Graph alignment: MAGNA++ [7]

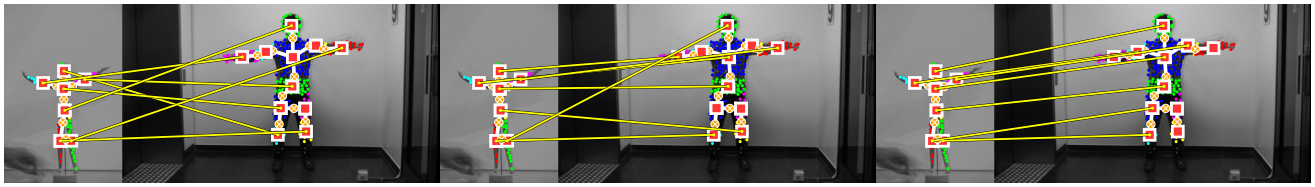

(d) Proposed $\mathcal{F}$ to TM [3] (e) Proposed $\mathcal{F}$ to HGM [8] (f) Proposed $\mathcal{F}$ to BCAGM+MP [6]

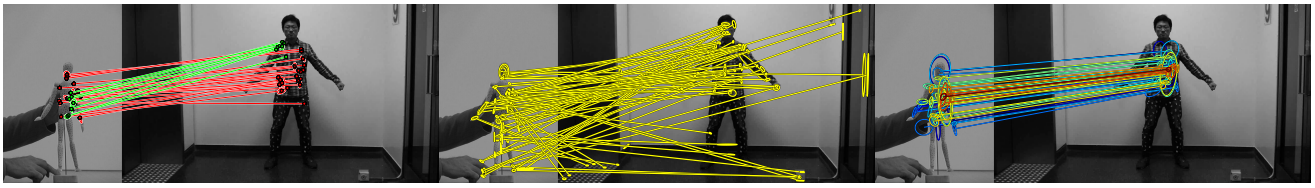

(g) Appearance feature matching: ACC [1] (h) Appearance feature matching: RRWM [4] (i) Appearance feature matching: PGM [2]

Figure 4. Experiments on real image datasets: puppet *vs.* human full body (best viewed in colour).

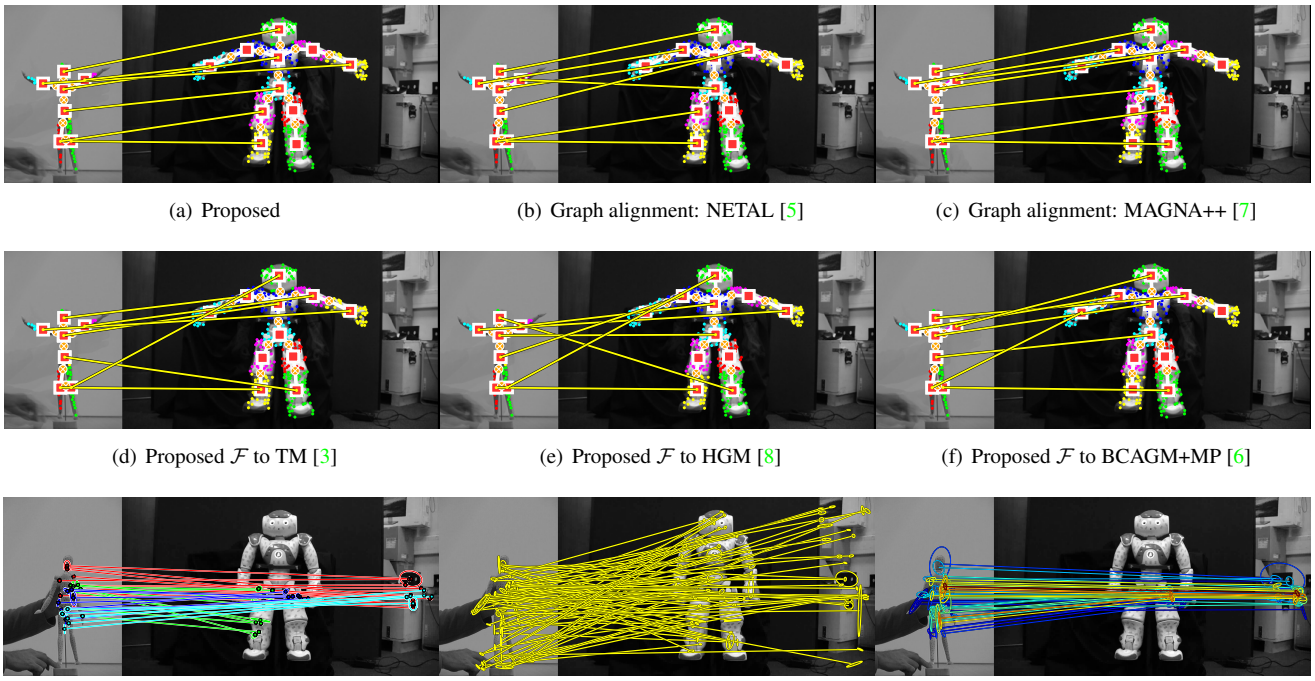

(a) Proposed (b) Graph alignment: NETAL [5] (c) Graph alignment: MAGNA++ [7]

(d) Proposed $\mathcal{F}$ to TM [3] (e) Proposed $\mathcal{F}$ to HGM [8] (f) Proposed $\mathcal{F}$ to BCAGM+MP [6]

(g) Appearance feature matching: ACC [1] (h) Appearance feature matching: RRWM [4] (i) Appearance feature matching: PGM [2]

Figure 5. Experiments on real image datasets: puppet *vs.* humanoid NAO full body (best viewed in colour).

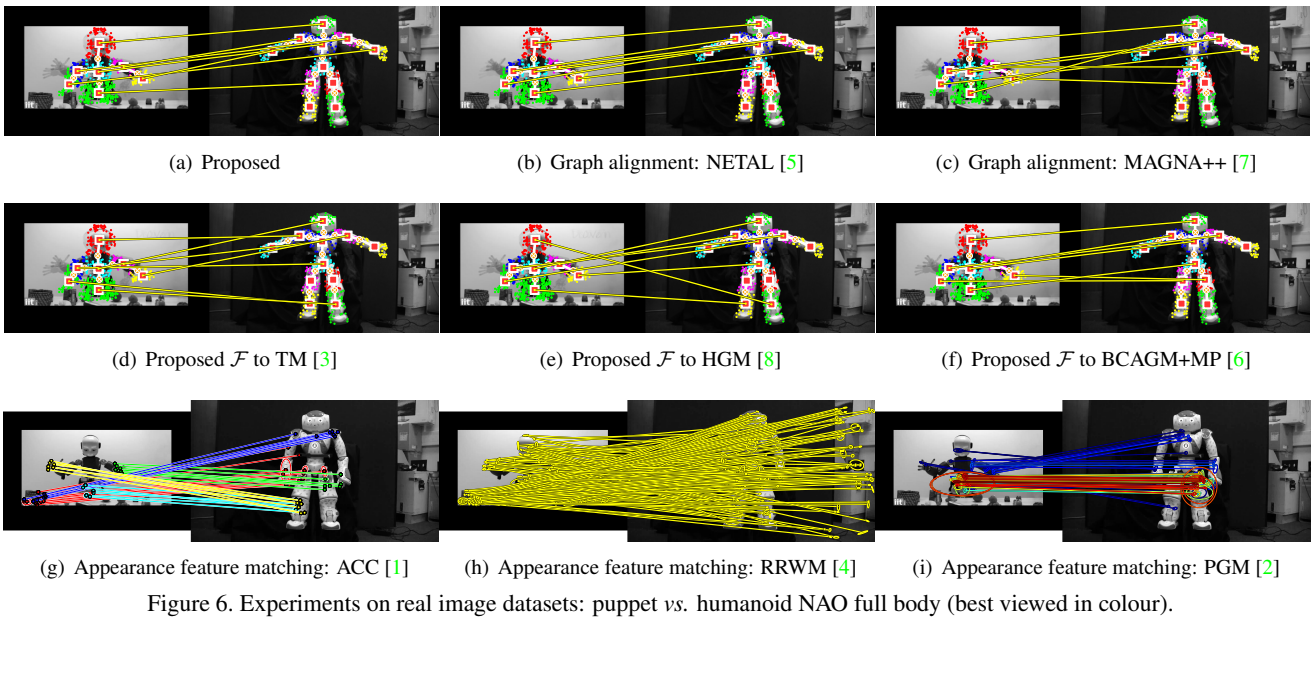

(a) Proposed (b) Graph alignment: NETAL [5] (c) Graph alignment: MAGNA++ [7]

(d) Proposed $\mathcal{F}$ to TM [3] (e) Proposed $\mathcal{F}$ to HGM [8] (f) Proposed $\mathcal{F}$ to BCAGM+MP [6]

(g) Appearance feature matching: ACC [1] (h) Appearance feature matching: RRWM [4] (i) Appearance feature matching: PGM [2]

Figure 6. Experiments on real image datasets: puppet *vs.* humanoid NAO full body (best viewed in colour).

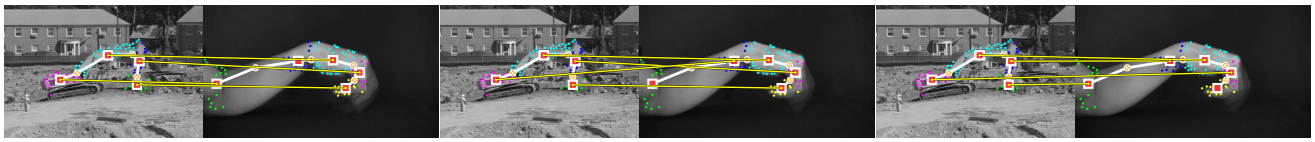

(a) Proposed (b) Graph alignment: NETAL [5] (c) Graph alignment: MAGNA++ [7]

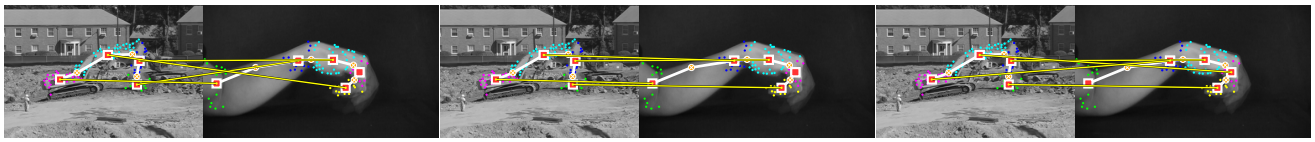

(d) Proposed $\mathcal{F}$ to TM [3] (e) Proposed $\mathcal{F}$ to HGM [8] (f) Proposed $\mathcal{F}$ to BCAGM+MP [6]

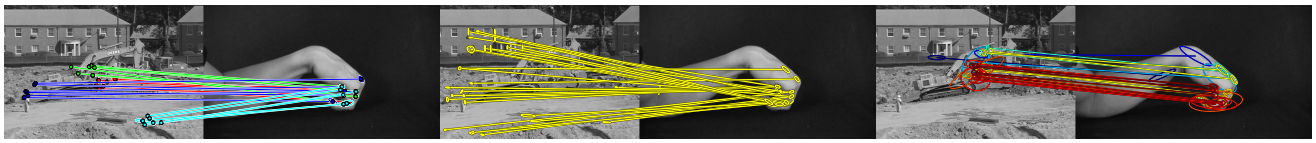

(g) Appearance feature matching: ACC [1] (h) Appearance feature matching: RRWM [4] (i) Appearance feature matching: PGM [2]

Figure 7. Experiments on real image datasets: yellow crane *vs.* digging arm (best viewed in colour).

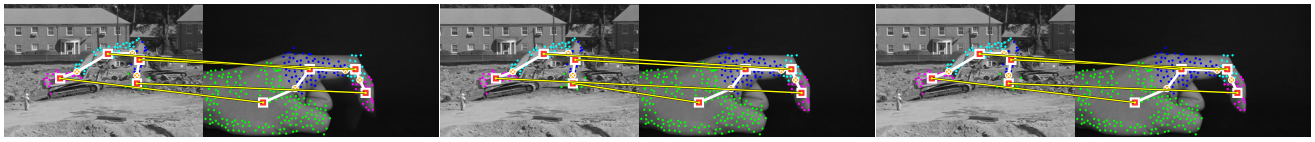

(a) Proposed (b) Graph alignment: NETAL [5] (c) Graph alignment: MAGNA++ [7]

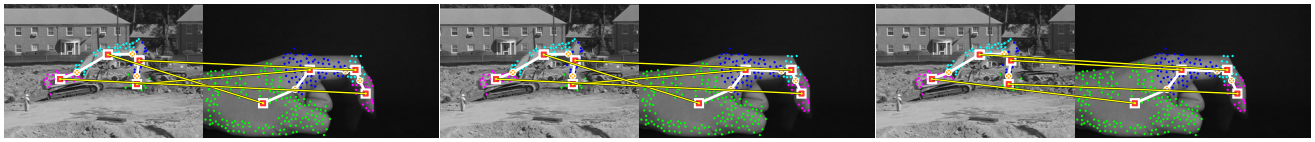

(d) Proposed $\mathcal{F}$ to TM [3] (e) Proposed $\mathcal{F}$ to HGM [8] (f) Proposed $\mathcal{F}$ to BCAGM+MP [6]

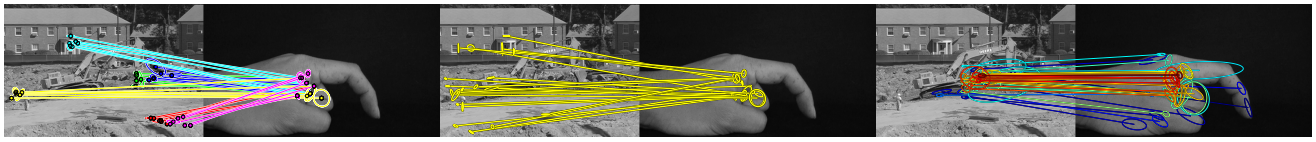

(g) Appearance feature matching: ACC [1] (h) Appearance feature matching: RRWM [4] (i) Appearance feature matching: PGM [2]

Figure 8. Experiments on real image datasets: yellow crane *vs.* digging finger (best viewed in colour).

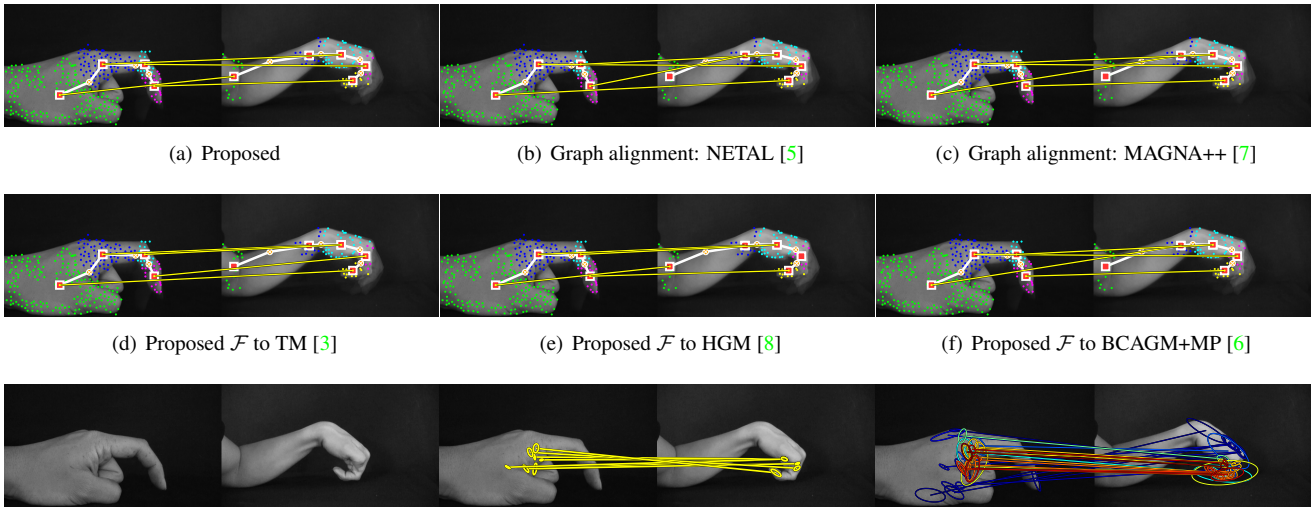

(a) Proposed (b) Graph alignment: NETAL [5] (c) Graph alignment: MAGNA++ [7]

(d) Proposed $\mathcal{F}$ to TM [3] (e) Proposed $\mathcal{F}$ to HGM [8] (f) Proposed $\mathcal{F}$ to BCAGM+MP [6]

(g) Appearance feature matching: ACC [1] (h) Appearance feature matching: RRWM [4] (i) Appearance feature matching: PGM [2]

Figure 9. Experiments on real image datasets: digging finger *vs.* digging arm (best viewed in colour).

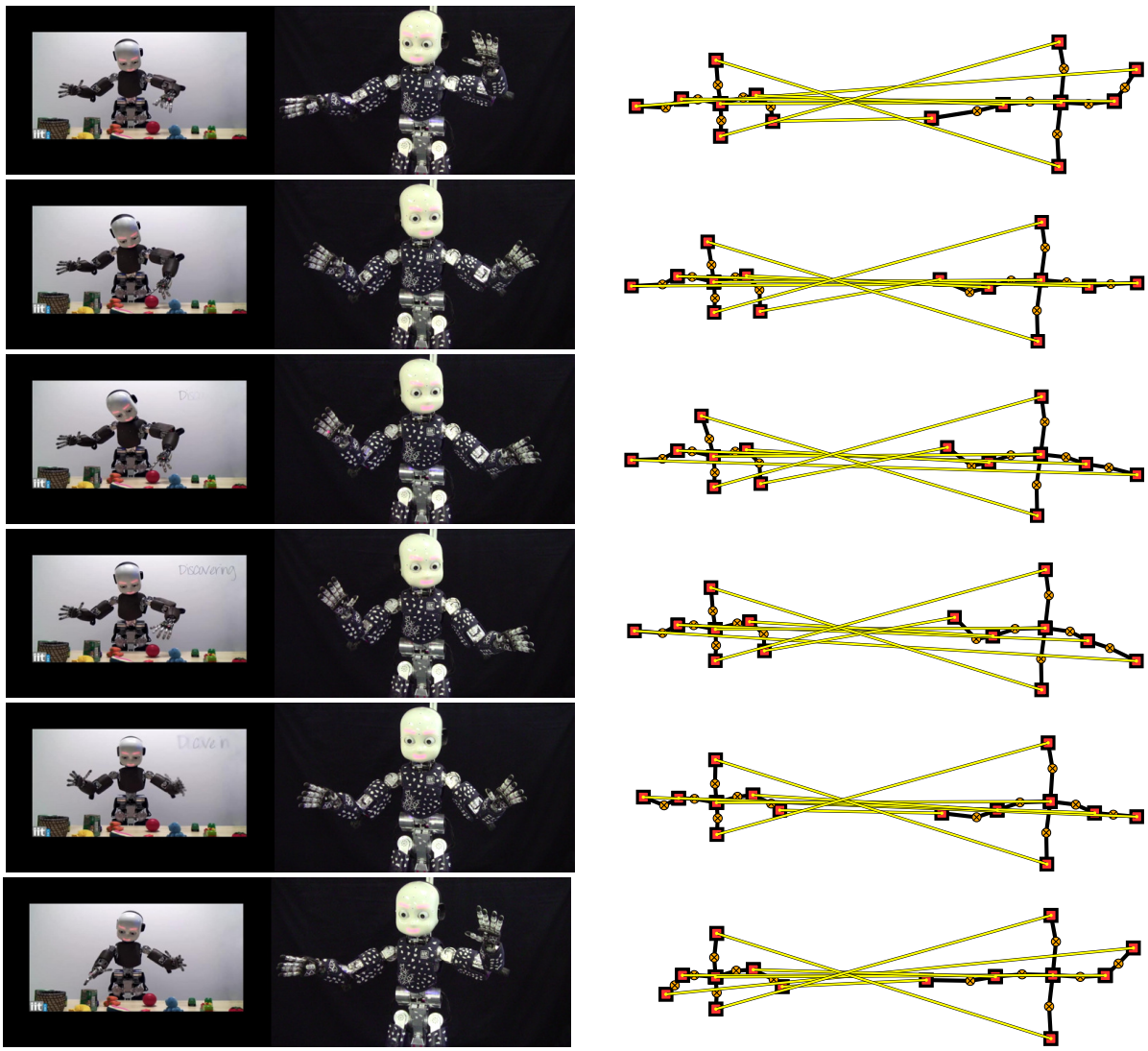

Figure 10. Sequential matches of iCub body sequence and iCub dancing sequence. The matches are upside-down, as the left iCub is moving its hands downwards, whilst the right iCub is waving its hands upwards. This shows that the combinatorial motion term can distinguish motion directions. (best viewed in colour).

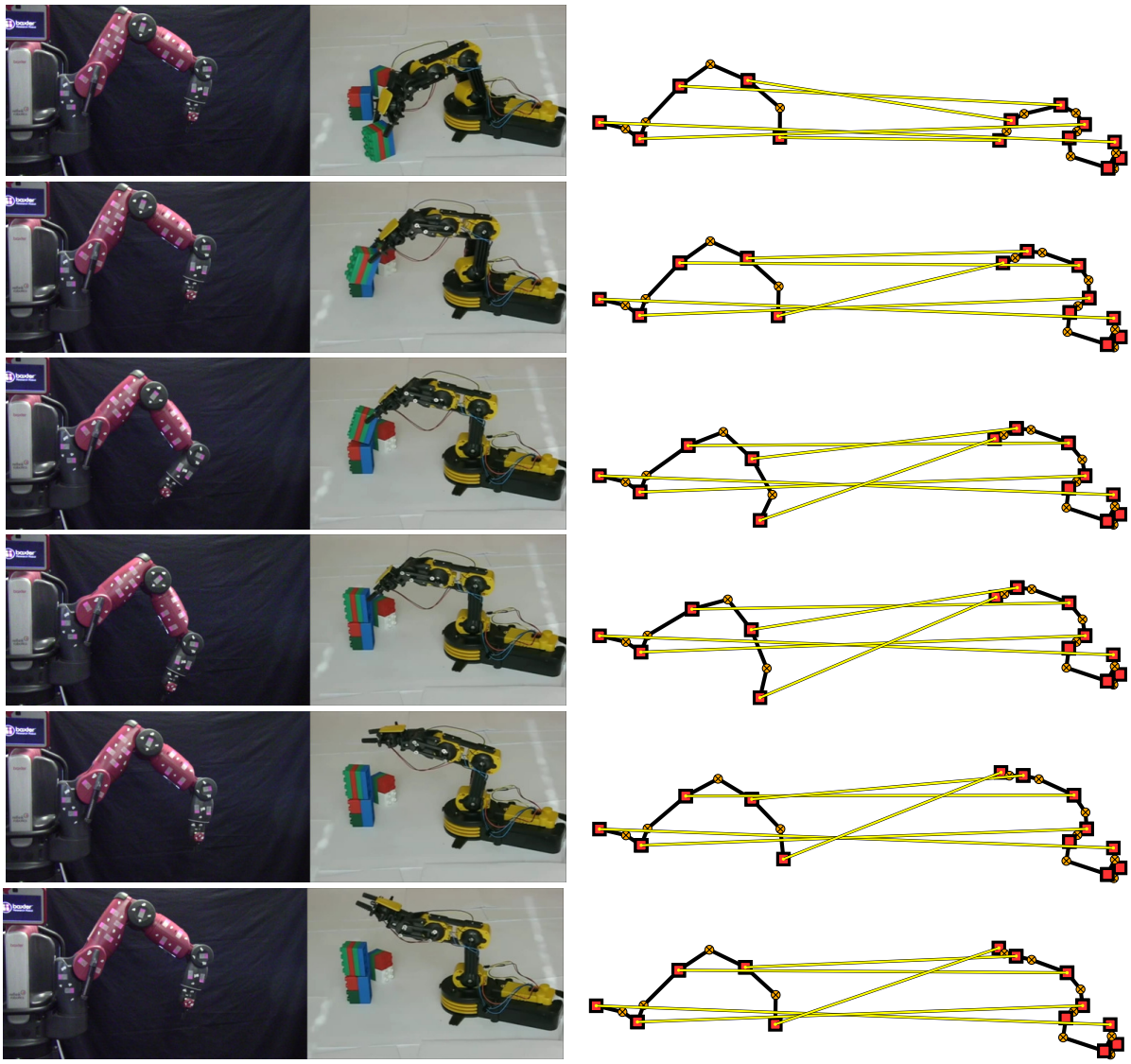

Figure 11. Sequential matches of Baxter arm and OWI-535 Robotic Arm Edge sequence. The matches are leftside-right. This also shows that the combinatorial motion term can distinguish motion directions. (best viewed in colour).

References

[1] M. Cho, J. Lee, and K. M. Lee. Feature Correspondence and Deformable Object Matching via Agglomerative Correspondence Clustering. In *ICCV*, pages 1280–1287, 2009. 2, 3, 4, 5, 6

[2] M. Cho and K. M. Lee. Progressive graph matching: Making a move of graphs via probabilistic voting. In *CVPR*, pages 398–405, 2012. 1, 2, 3, 4, 5, 6

[3] O. Duchenne, F. Bach, I.-S. Kweon, and J. Ponce. A Tensor-Based Algorithm for High-Order Graph Matching. *IEEE Trans. on PAMI*, 33(12):2383–2395, Dec 2011. 2, 3, 4, 5, 6

[4] J. Lee, M. Cho, and K. M. Lee. Hyper-graph Matching via Reweighted Random Walks. In *CVPR*, pages 1633–1640, 2011. 2, 3, 4, 5, 6

[5] B. Neyshabur, A. Khadem, S. Hashemifar, and S. S. Arab. NETAL: A new graph-based method for global alignment of protein-protein interaction networks. *Bioinformatics*, 29(13):1654–1662, 2013. 2, 3, 4, 5, 6

[6] Q. Nguyen, A. Gautier, and M. Hein. A Flexible Tensor Block Coordinate Ascent Scheme for Hypergraph Matching. In *CVPR*, pages 5270–5278, 2015. 2, 3, 4, 5, 6

[7] V. Vijayan, V. Saraph, and T. Milenković. MAGNA++: Maximizing Accuracy in Global Network Alignment via both node and edge conservation. *Bioinformatics*, 31(14):2409–2411, 2015. 2, 3, 4, 5, 6

[8] R. Zass and A. Shashua. Probabilistic Graph and Hypergraph Matching. In *CVPR*, pages 1–8, 2008. 2, 3, 4, 5, 6